Polskie Towarzystwo Materiałów Kompozytowych
Polish Society of Composite Materials

26: 3 (2026) 179–191

COMPOSITES THEORY AND PRACTICE

ISSN (online): 2299-128X

Eduard Lysenkov[1, *] (ID: 0000-0002-1369-4609), Sergiy Bilyi[1] (ID: 0000-0002-6967-9037), Valeriy Klepko[2] (ID: 0000-0001-8089-8305)

[1] *Petro Mohyla Black Sea National University, 54003, 68 Desantnykiv St., 10, Mykolaiv, Ukraine*
[2] *Institute of Macromolecular chemistry NAS of Ukraine 48, Kharkivske shose, Kyiv, 02155, Ukraine*
* *Correspondence*: ealysenkov@ukr.net

Received (Otrzymano) 30.06.2026
Published on-line (Opublikowano) 30.09.2026

EFFECT OF MIXING TIME ON ELECTRICAL AND DIELECTRIC PROPERTIES OF PEO/OMMT NANOCOMPOSITES

https://doi.org/10.62753/ctp.2026.03.3.3

The influence of the mixing time on the electrical and dielectric properties of poly(ethylene oxide)/organically modified montmorillonite (PEO/OMMT) nanocomposites prepared using a piston-type extrusion process was investigated by dielectric spectroscopy in the frequency range from 100 Hz to 100 kHz. The AC conductivity spectra were analyzed using the Jonscher universal power law, while impedance data were interpreted by means of equivalent-circuit modeling. Dielectric relaxation behavior was evaluated from the frequency dependences of the dielectric loss tangent. The results revealed a non-monotonic dependence of the electrical characteristics on the mixing time. The DC conductivity increased by more than two orders of magnitude and reached a maximum at 3 min of processing, whereas the bulk resistance and effective relaxation time exhibited corresponding minima. Analysis of the loss tangent spectra showed a significant shift in the characteristic relaxation frequency toward higher frequencies with increasing conductivity. Scaling analysis performed in normalized coordinates showed that the conductivity, impedance, and dielectric relaxation parameters collapse onto a common master curve, indicating that their evolution is governed by a common structural mechanism. The observed behavior was attributed to the competition between the development and subsequent reorganization of the dispersed OMMT structure during mechanical processing. An optimal mixing time of approximately 3 min was identified, corresponding to the most favorable electrical and dielectric performance of the nanocomposites.

Keywords: PEO/OMMT nanocomposites; dielectric spectroscopy; AC conductivity; dielectric relaxation; Jonscher model; scaling behavior

INTRODUCTION

Polymer nanocomposites containing nanoscale fillers have attracted considerable attention owing to their ability to combine the processability of polymers with the unique functional properties of nanostructured materials [1, 2]. The incorporation of layered silicates, carbon nanomaterials, metal nanoparticles, and other nanoscale additives enables substantial modification of the mechanical, thermal, barrier, electrical, and dielectric characteristics of polymer matrices. Among these systems, polymer/clay nanocomposites remain one of the most extensively studied classes of nanostructured materials due to their relatively low cost, high aspect ratio of the filler, and the possibility of tailoring their structure through appropriate processing techniques [3, 4].

Organically modified montmorillonite (OMMT) is widely used as a nanofiller in polymer matrices because its layered structure provides a large specific surface area and promotes the formation of

 All rights reserved

extensive interfacial regions [5, 6]. Depending on the degree of clay dispersion, intercalation, and exfoliation, OMMT may significantly affect the morphology and physical properties of polymer nanocomposites [7]. The final performance of such materials is therefore strongly governed not only by the filler concentration but also by the structural state achieved during processing [8, 9].

Poly(ethylene oxide) (PEO) represents an attractive polymer matrix for the preparation of nanocomposites owing to its flexibility, semicrystalline nature, ion-conducting ability, and broad range of technological applications [10, 11]. The interaction between the PEO chains and silicate layers may alter chain mobility, crystallization behavior, charge transport processes, and interfacial polarization phenomena [12, 13]. As a consequence, PEO/OMMT nanocomposites have emerged as promising materials for applications requiring controlled electrical and dielectric properties.

Dielectric spectroscopy is a powerful tool for investigating the relationship between the structure and electrical response in heterogeneous polymer systems. In addition to providing information on dielectric permittivity and electrical conductivity, this technique enables the analysis of polarization mechanisms, relaxation processes, and charge transport phenomena occurring over a wide range of frequencies [14]. Since dielectric properties are highly sensitive to the dispersion state of nanofillers and the characteristics of interfacial regions, dielectric spectroscopy is particularly useful for studying the structural evolution of polymer/clay nanocomposites [15].

Sengwa et al. investigated the dielectric behavior of montmorillonite-filled PVA/PEO blend nanocomposites and showed that the dielectric response is strongly affected by the degree of clay dispersion and polymer–clay interactions [16]. The authors reported significant changes in dielectric relaxation behavior and electrical conductivity associated with intercalated and exfoliated clay structures. Anwar et al. studied polymer nanocomposites containing organically modified montmorillonite and showed that exfoliated structures exhibit substantially higher dielectric permittivity than their intercalated counterparts [17]. The enhancement was attributed to an increased interfacial area and stronger Maxwell–Wagner–Sillars polarization arising from the polymer–clay interfaces. Noda et al. employed dielectric relaxation spectroscopy to correlate the morphology of nylon 6/clay nanocomposites with their electrical response [18]. The study demonstrated that dielectric parameters are highly sensitive to the degree of clay exfoliation and can be used to monitor structural change during processing.

Although numerous studies have investigated the influence of OMMT on the dielectric properties of polymer nanocomposites [15-19], considerably less attention has been devoted to the effect of the processing-induced structural response on the electrical response of PEO/OMMT systems. In particular, the relationship between the mixing conditions, charge transport characteristics, dielectric relaxation behavior, and impedance response remains insufficiently understood. Since the degree of clay dispersion may evolve continuously during processing, identifying the corresponding changes in electrical and dielectric properties is essential for establishing structure–property relationships in these materials.

The present work aims to investigate the influence of the mixing time on the electrical and dielectric behavior of PEO/OMMT nanocomposites prepared using a piston-type extrusion process. The frequency-dependent conductivity, dielectric response, and impedance characteristics were analyzed using the Jonscher power law, equivalent-circuit modeling, and dielectric relaxation analysis. Particular attention was focused on establishing correlations between the charge transport, interfacial polarization, and the structural evolution induced by the mechanical dispersion of OMMT within the polymer matrix.

MATERIALS AND METHODS

Materials

Poly(ethylene oxide) (PEO) with a molecular weight of 1000 g/mol was used as the polymer matrix in the present study. The polymer was supplied by Aldrich and used without additional purification.

Organomodified montmorillonite (OMMT) was used as the layered silicate nanofiller. The MMT was obtained from the Pygevskii deposit

 All rights reserved

(Ukraine). The OMMT was prepared by ion-exchange reactions. Long chain cetyltrimethylammonium bromide ions ($C_{16}H_{33}N(CH_3)_3^+ \cdot Br^-$, CTAB, Merck) were chosen as the swelling agent for intercalation into the MMT platelets [9].

PEO/OMMT nanocomposites containing 5 wt% OMMT were prepared using shear-assisted piston extrusion mixing. For all the experiments, the total mass of the processed material was maintained at 2 g in order to minimize the influence of the sample mass on the energetic characteristics of the process.

Prior to processing, the required amounts of PEO and OMMT were mechanically premixed to obtain an approximately uniform initial distribution of the layered silicate within the polymer matrix.

Preparation of nanocomposites

The shear-assisted melt mixing of the PEO/OMMT nanocomposites was performed utilizing a laboratory piston extrusion system equipped with a rotating mixing element [20]. The extrusion chamber had an internal diameter of 50 mm and a working length of 30 mm. The mixing system operated under conditions combining axial compression and rotational shear deformation of the polymer melt.

The rotational speed of the mixing element was maintained at 2650 rpm, while the processing temperature was controlled at approximately 80 °C. The total processing time varied from 1 to 15 min with a step of 2 min, similar to ultrasonic treatment experiments.

During processing, the polymer/clay mixture experienced intensive viscous shear and extensional deformation, leading to redistribution and partial disintegration of OMMT tactoids within the molten PEO matrix. The geometry of the mixing zone and the imposed rotational motion generated nonuniform shear fields contributing to the structural changes of the nanocomposite system.

After processing, the obtained samples were removed from the extrusion chamber, cooled to room temperature under ambient conditions, and stored in sealed containers prior to characterization.

Characterization methods

The study of the electrical and dielectric properties was carried out by means of dielectric relaxation spectroscopy with an E7-20 impedance meter. The sample was placed between the electrodes of the cell, while its real (Z') and imaginary (Z'') parts of the impedance were measured. The dielectric characteristics were calculated from the impedance values. The measurements were conducted at room temperature in the frequency range of 100 Hz – 100 kHz. The constant gap between the electrodes was 100 μm.

RESULTS AND DISCUSSION

AC conductivity and charge transport mechanism

Fig. 1 shows the frequency dependences of the AC conductivity for the PEO/OMMT nanocomposites prepared at different mixing times. The conductivity spectra exhibit characteristic behavior commonly observed in disordered ionic conductors [21]. At low frequencies, the conductivity remains nearly frequency-independent, corresponding to the DC conductivity plateau, whereas at higher frequencies a gradual increase in conductivity is observed owing to the dispersive contribution associated with charge carrier hopping and localized transport processes [22].

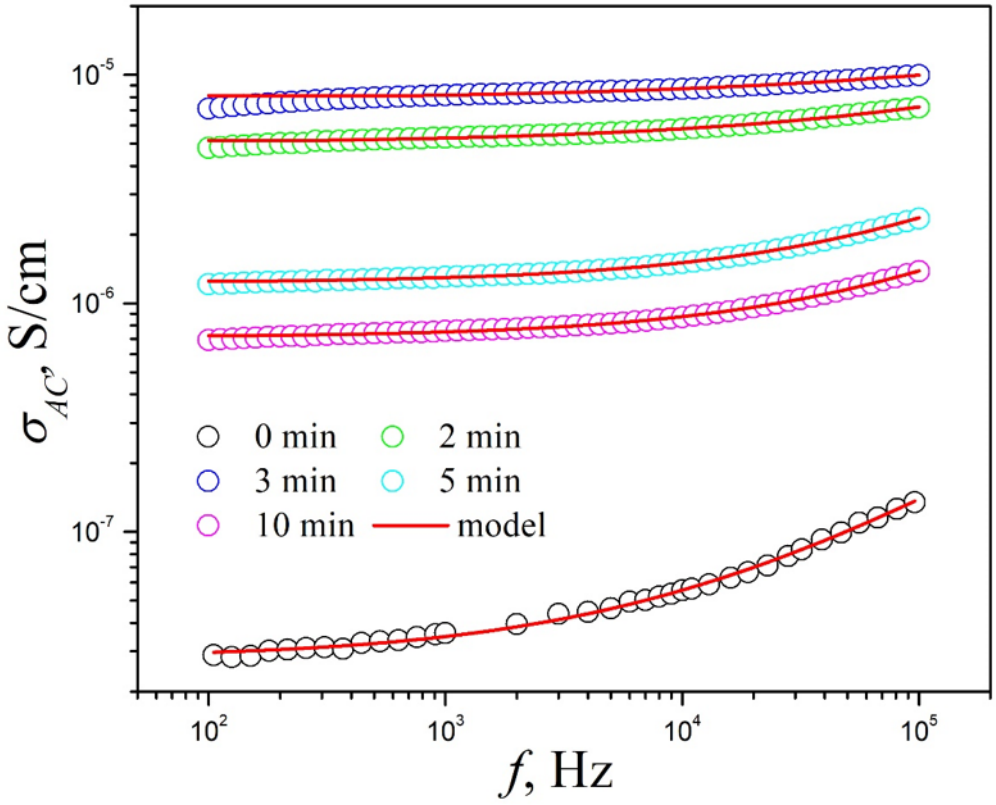

Fig. 1. Frequency dependence curves of electrical conductivity at alternating current for PEO/OMMT nanocomposites produced using different mixing times. Solid line is Jonscher model (Eq. 1)

The experimental spectra were analyzed using the Jonscher universal power law [23, 24]:

$$\sigma(\omega) = \sigma_{DC} + \sigma_{AC} = \sigma_{DC} + A\omega^n \quad (1)$$

where σ_{DC} is the DC conductivity, ω is the cyclic frequency of the applied electric field ($\omega=2\pi f$), A is the temperature- and structure-dependent constant, and n is the frequency exponent characterizing the charge transport mechanism.

Table 1. **Jonscher model parameters (Eq. 1)**

***t*, min**	**σ_{DC}, S/cm**	***A*, S/cm**	***n***
0	$2.8\cdot10^{-8}$	$3.4\cdot10^{-11}$	0.60
2	$5.0\cdot10^{-6}$	$6.4\cdot10^{-9}$	0.43
3	$7.8\cdot10^{-6}$	$1.6\cdot10^{-8}$	0.37
5	$1.2\cdot10^{-6}$	$3.2\cdot10^{-10}$	0.57
10	$7.1\cdot10^{-7}$	$1.5\cdot10^{-10}$	0.62

 All rights reserved

Table 1 presents the fitting results, which reveal a substantial dependence of the electrical conductivity on the mixing time. The DC conductivity increases from $2.8 \cdot 10^{-8}$ S/cm for the untreated system to $5.0 \cdot 10^{-6}$ S/cm after 2 min of mixing and reaches a maximum value of $7.8 \cdot 10^{-6}$ S/cm at 3 min. Further processing results in a decrease in conductivity to $7.1 \cdot 10^{-7}$ S/cm after 10 min.

The initial growth in conductivity specifies progressive improvement in the dispersion state of OMMT within the polymer matrix. Mechanical treatment promotes the breakup of tactoidal clay aggregates and increases the interfacial area between the polymer and the layered silicate [8]. As a result, the mobility of charge carriers and the continuity of conductive pathways are enhanced [25]. The conductivity maximum observed at 3 min suggests the formation of the most favorable microstructure for charge transport.

Prolonged mixing beyond 3 min leads to a reduction in conductivity, indicating that further mechanical treatment does not improve the conductive network. Instead, structural reorganization processes may become dominant, resulting in partial loss of the highly conductive state achieved during the earlier stages of dispersion. Similar non-monotonic behavior has previously been observed in the structural and thermal characteristics of PEO/OMMT systems [26], suggesting that the electrical response is strongly governed by the change in the nanocomposite microstructure during processing.

Additional insight into the charge transport mechanism can be obtained from frequency exponent n. The exponent decreases from 0.60 for the untreated material to 0.37 at 3 min of mixing, followed by an increase to 0.62 after 10 min. The minimum n value coincides with the maximum conductivity. This behavior indicates that the transport process becomes increasingly non-Debye-like as the dispersion state improves and reaches its highest structural complexity [22]. The subsequent increase in n at longer mixing times suggests a narrowing of the distribution of conductive environments and a partial loss of the heterogeneous structure responsible for enhanced charge transport.

The simultaneous occurrence of the conductivity maximum and the minimum value of the Jonscher exponent shows that the electrical response of the PEO/OMMT nanocomposites is controlled not only by the concentration of charge carriers but also by the structural organization of the conductive pathways formed during the dispersion process. Consequently, the observed changes in the conductivity spectra reflect the competition between structure development and structure reorganization occurring during mechanical treatment [21].

Impedance analysis and equivalent circuit modeling

The impedance response of the PEO/OMMT nanocomposites was further analyzed using Nyquist plots in order to elucidate the influence of the mixing time on the charge transport and interfacial polarization processes (Fig. 2). All the samples exhibited depressed semicircular arcs, indicating a deviation from ideal Debye behavior and the presence of a distribution of relaxation times associated with structural heterogeneity of the nanocomposite system.

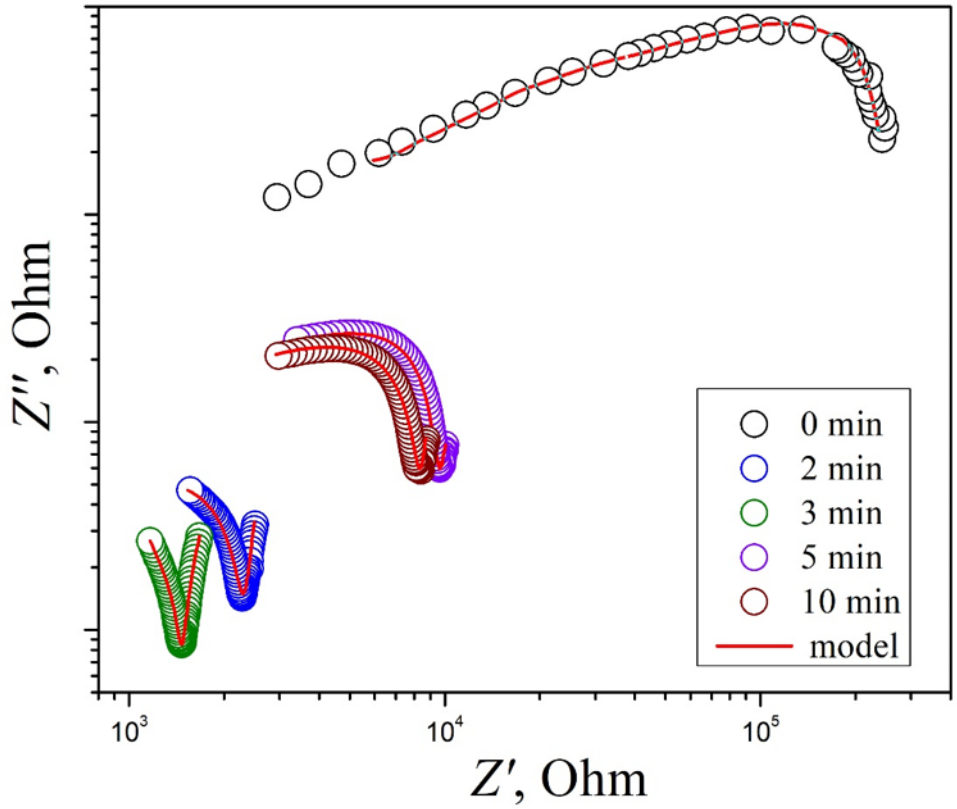

Fig. 2. Nyquist plots of PEO/OMMT nanocomposites for different mixing times. Solid lines display fitting using an equivalent circuit

To quantitatively describe the impedance spectra, the experimental data were fitted utilizing an equivalent circuit, shown in Fig. 3. This equivalent circuit is typical for nanofilled PEO-based systems [27].

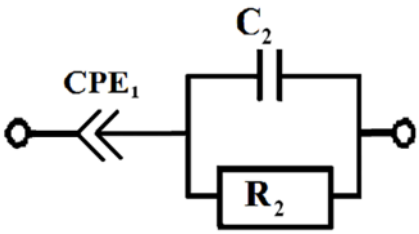

Fig. 3. Equivalent circuit for modeling impedance spectra of PEO/OMMT nanocomposites

This circuit provided the best agreement with the experimental data over the entire investigated frequency range. The parallel R_2C_2 branch represents the bulk electrical response of the composite, whereas the CPE accounts for non-ideal capacitive behavior originating from structural disorder and interfacial heterogeneity. According to the given equivalent circuit, the total impedance of the system will be written as:

$$Z = \frac{1}{(i\omega)^{\alpha_1} C_1} + \frac{1}{i\omega C_2 + \frac{1}{R_2}}, \qquad (2)$$

where C_1 is the capacitance; α is the exponential exponent that characterizes the phase deviation; R_2 is the total volume resistance and C_2 is the capacitance of the material. The modelling results are presented in Table 2.

 All rights reserved

Table 1. **Fitting parameters of model described by Eq. 2**

Mixing time, min	Interfacial layer			Bulk phase	
	C_1, μF	n	D	R_2, kΩ	C_2, μF
0	2360.0	0.77	2.29	236.0	4.2
2	24.6	0.57	2.74	2.3	37.4
3	11.2	0.52	2.92	1.4	60.5
5	335.5	0.63	2.55	8.4	16.3
10	413.4	0.65	2.57	9.8	15.9

Bulk resistance R_2, obtained from the fitting procedure, exhibits a pronounced dependence on the mixing time. The resistance decreases from 236 kΩ for the untreated material to 2.3 kΩ after 2 min of mixing and reaches a minimum value of 1.4 kΩ at 3 min. Further mixing results in a rise in the resistance to 9.8 kΩ after 10 min. This behavior is fully consistent with the variation in the DC conductivity determined from the Jonscher model and confirms the existence of an optimal processing time at which the charge transport through the composite is maximized.

The substantial reduction in R_2 during the initial stages of processing demonstrates significant improvement in the electrical connectivity of the system. Mechanical dispersion promotes the breakdown of OMMT tactoids and increases the effective interfacial area between the polymer matrix and the clay particles. These structural changes facilitate charge transport and reduce the resistance of the bulk material [28]. The minimum resistance observed at 3 min suggests that the nanocomposite reaches its most favorable electrically conductive state employing this processing parameter.

The depressed nature of the impedance arcs required the introduction of a constant phase element instead of an ideal capacitor. Such behavior is commonly associated with a broad distribution of local electrical environments and relaxation times [29]. In heterogeneous polymer nanocomposites, deviations from ideal capacitive behavior may arise from variations in local conductivity, differences in interfacial polarization intensity, and structural disorder associated with the dispersion state of the filler [30].

Analysis of the CPE exponent revealed a non-monotonic dependence on the mixing time. The exponent decreases during the initial stages of processing and reaches its minimum value at approximately 3 min, followed by growth at longer mixing times. Since lower values of the CPE exponent correspond to a broader distribution of relaxation times and a higher degree of electrical heterogeneity [31], the observed minimum shows the formation of the most structurally complex state of the nanocomposite. The subsequent rise in the exponent suggests partial structural reorganization and a reduction in heterogeneity.

The impedance spectroscopy results therefore support the conclusions obtained from the conductivity analysis. Both approaches consistently indicate that the change in the electrical properties is governed by changes in the microstructure of the dispersed clay phase. The simultaneous occurrence of the maximum conductivity and minimum bulk resistance at 3 min demonstrates that this processing parameter provides the most efficient balance between clay intercalation, interfacial development, and charge transport within the PEO/OMMT nanocomposite.

Assuming a fractal interpretation of the CPE response, exponent n can be qualitatively related to an effective fractal dimension according to $D = 1+1/n$ [32]. Within this framework, the minimum of n observed at 3 min suggests the maximum structural complexity of the interfacial network.

Dielectric relaxation analysis

The dielectric response of the PEO/OMMT nanocomposites was analyzed by means of the frequency dependences of the dielectric loss

 All rights reserved

tangent (Fig. 4). Among all the dielectric characteristics investigated in the present work, the loss tangent spectra exhibited the most relaxation features within the accessible frequency range and therefore provide the most reliable basis for evaluating the response of relaxation processes during mixing.

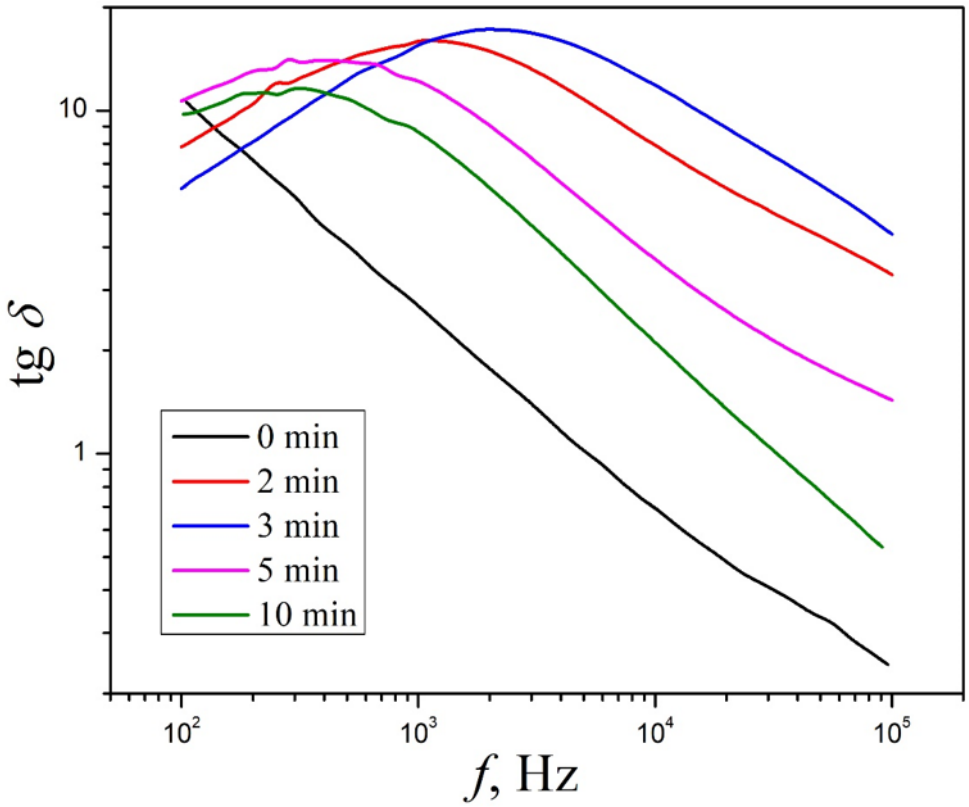

Fig. 4. Frequency dependences of dielectric loss tangent of PEO/OMMT nanocomposites

The frequency dependences of the real and imaginary parts of the dielectric permittivity and electric modulus demonstrated the expected dispersive behavior characteristic of heterogeneous polymer nanocomposites. However, no distinct relaxation maxima were observed within the investigated frequency window. This shows that the characteristic frequencies of the dominant relaxation processes are located partially outside the experimental range and only the corresponding low-frequency or high-frequency flanks are captured in the measured spectra. Under such conditions, direct determination of the relaxation parameters from the permittivity or modulus representations becomes unreliable. In contrast, the loss tangent spectra exhibit well-defined maxima for all the investigated samples, enabling a consistent comparative analysis of dielectric relaxation behavior.

The observed loss peaks are attributed to polarization processes occurring in the heterogeneous PEO/OMMT system. Considering the relatively high clay loading and the significant contrast between the electrical properties of the polymer matrix and the dispersed silicate phase, the relaxation behavior is predominantly associated with interfacial polarization phenomena [33]. Such processes arise from the accumulation of charge carriers at the interfaces and are highly sensitive to the dispersion state of the layered silicate.

A significant shift in the loss peak position with mixing time is observed. The characteristic frequency corresponding to the maximum of the loss tangent increases for the untreated material and reaches the maximum after 3 min of processing. Further mixing results in a decline in the peak frequency. The non-monotonic variation of

 All rights reserved

the characteristic frequency indicates substantial changes in the dynamics of charge accumulation and relaxation processes during structural development of the nanocomposite.

To quantify these changes, an effective relaxation time was estimated according to

$$\tau_{eff} = \frac{1}{2\pi f_{\max}} \tag{3}$$

where f_{max} is the frequency corresponding to the maximum of the loss tangent spectrum [34].

The calculated relaxation time decreases substantially during the initial stages of mixing, reaching its minimum value at 3 min, and subsequently grows at longer processing times. This behavior mirrors the change in the DC conductivity and bulk resistance obtained from conductivity and impedance analyses. The coincidence of the conductivity maximum, resistance minimum, and relaxation time minimum strongly suggests that all three parameters are governed by the same structural transformations occurring during the dispersion of OMMT in the polymer matrix.

The reduction in the effective relaxation time during the initial mixing stage indicates a faster dielectric response of the system. As the clay tactoids become progressively dispersed and the interfacial area increases, charge redistribution processes occur more rapidly, resulting in a shift in the relaxation peak toward higher frequencies. The subsequent growth in relaxation time observed after prolonged mixing suggests a partial loss of this highly responsive state as a consequence of structural reorganization within the composite.

An important observation is that the characteristic frequency exhibits a considerably larger relative variation than the conductivity. While the conductivity changes by approximately two orders of magnitude, the relaxation frequency shifts by nearly two decades. This high sensitivity demonstrates that dielectric relaxation analysis provides valuable information regarding subtle structural changes that may not be fully reflected by conductivity measurements alone.

Overall, the dielectric relaxation analysis confirms that the electrical response of the PEO/OMMT nanocomposites is strongly affected by the variation in the interfacial structure during mechanical processing. The maximum relaxation frequency and the corresponding minimum effective relaxation time observed at 3 min show that this processing condition yields the most dynamically responsive dielectric structure among the investigated samples.

Evolution of electrical and dielectric properties with mixing time

To identify possible correlations between the electrical and dielectric characteristics of the PEO/OMMT nanocomposites, the results obtained from the conductivity analysis, impedance spectroscopy, and dielectric relaxation measurements were represented in normalized coordinates as a function of mixing time (Fig. 5). For quantities (P) exhibiting a maximum, normalization was performed as P/P_{max}, whereas results characterized by a minimum were transformed as P_{min}/P. Such normalization eliminates the differences in magnitude and units, allowing direct comparison of the change in various physical quantities.

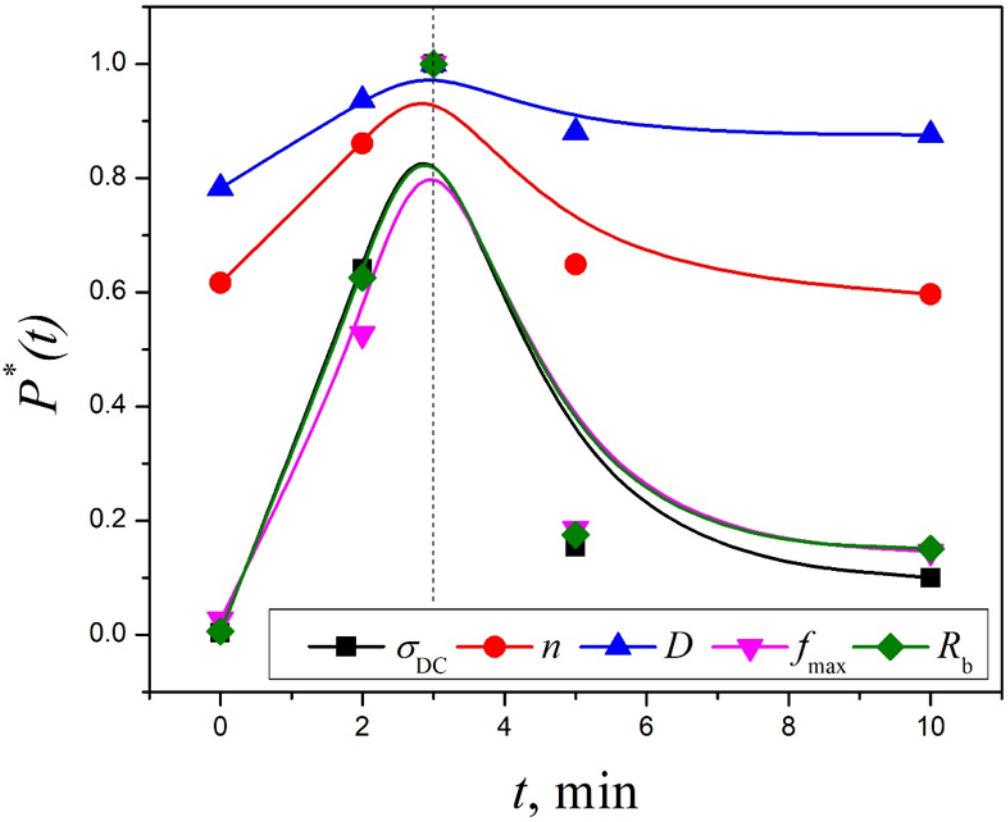

Fig. 5. Electrical and dielectric characteristics of PEO/OMMT nanocomposites in normalized coordinates as a function of mixing time

The normalized dependences reveal clear scaling behavior. Despite being derived from different experimental techniques and describing different aspects of the electrical response, all the investigated parameters collapse onto a common master curve. In particular, the DC conductivity, loss tangent maximum, characteristic relaxation frequency, bulk resistance, and other derived electrical parameters exhibit extrema at approximately the same mixing time, corresponding to 3 min of processing.

The observed collapse suggests that the variation in the electrical properties originates from a common underlying structural mechanism. Although the considered parameters characterize different physical phenomena, including the charge transport, dielectric losses, interfacial polarization, and impedance response, their synchronized evolution demonstrates that these processes exhibit correlated behavior through the microstructural state of the nanocomposite.

The existence of a single master curve suggests that the mixing time acts as an effective control parameter for the development of the internal structure of the PEO/OMMT system. During the initial stage of processing, the progressive dispersion of OMMT tactoids and growth of the interfacial area lead to simultaneous enhancement of the conductivity, dielectric response, and polarization dynamics. As a consequence, all the normalized characteristics move toward their optimum values. At longer mixing times, structural reorganization processes become increasingly important, resulting in a coordinated drop in the electrical performance indicators and a departure from the optimum state.

Particularly noteworthy is the fact that the collapse is observed for parameters extracted from fundamentally different representations of the experimental data. The conductivity parameters originate from the Jonscher model, the resistance values are obtained from equivalent-circuit fitting of the impedance spectra, and the relaxation characteristics are derived from the dielectric loss measurements. The convergence of independently obtained results onto a common master curve suggests that they are governed by a common underlying structural process.

 All rights reserved

The data collapse in normalized coordinates observed in the present work indicates that the electrical response of PEO/OMMT nanocomposites can be described within a unified structural framework. The common extremum at approximately 3 min of mixing corresponds to the state of maximum electrical activity and dielectric responsiveness of the system. This finding supports the hypothesis that the electrical properties are controlled by the competition between structure development and subsequent structural reorganization occurring during mechanical dispersion of the layered silicate.

Overall, the scaling analysis demonstrates that the various electrical and dielectric characteristics do not evolve independently. Instead, they represent different manifestations of the same structural transformation process occurring within the nanocomposite during mixing.

CONCLUSIONS

The influence of the mixing time on the electrical and dielectric properties of PEO/OMMT nanocomposites prepared using a piston-type extrusion process was investigated by means of dielectric spectroscopy, conductivity analysis, and impedance spectroscopy.

The AC conductivity spectra were successfully described using the Jonscher power law. The DC conductivity exhibited a non-monotonic dependence on the mixing time. The variations in the Jonscher exponent indicate changes in the charge transport mechanism associated with structural modification of the nanocomposite.

Equivalent-circuit fitting of the impedance spectra revealed a satisfactory description of the impedance response of all the investigated samples. The bulk resistance decreased significantly during the initial stages of processing and reached a minimum value at 3 min of mixing, confirming the formation of the most electrically conductive structure under these conditions.

Dielectric relaxation behavior was evaluated from the frequency dependences of the loss tangent. Well-defined loss peaks were observed within the investigated frequency range, allowing determination of the characteristic relaxation frequency and effective relaxation time. The relaxation frequency reached a maximum value at 3 min of mixing, while the corresponding effective relaxation time exhibited a minimum, indicating the fastest dielectric response of the system.

Comparison of the parameters obtained from conductivity analysis, impedance spectroscopy, and dielectric relaxation measurements revealed a common extremum at approximately 3 min of mixing. The simultaneous occurrence of the conductivity maximum, bulk resistance minimum, maximum relaxation frequency, and minimum relaxation time shows a strong correlation between the charge transport, interfacial polarization, and structural evolution of the dispersed clay phase.

Scaling analysis performed in normalized coordinates showed that the electrical and dielectric characteristics collapse onto a common master curve. This behavior indicates that the observed changes in the electrical response are governed by a common structural mechanism associated with the development and subsequent reorganization of the OMMT network during processing.

The results show that dielectric spectroscopy combined with conductivity and impedance analysis provides a sensitive tool for monitoring the structural change of PEO/OMMT nanocomposites. An optimal mixing time of approximately 3 min was identified, corresponding to the most favorable state of the nanocomposite in terms of electrical conductivity and dielectric performance.

Funding declaration

The authors received no financial support for the research, authorship, and/or publication of this article.

REFERENCES

[1] Okamoto M., Polymer nanocomposites, Eng, 2023, 4, 457–479, https://doi.org/10.3390/eng4010028.

[2] Khdier H.M., Husham K.A.F., Shali W.M., Al-Atabi H.A., Interfacial effects on mechanical, thermal and electrical properties of polymer-based nanocomposites: A review, Ann Chim Sci Mater, 2024, 48, 857–869, https://doi.org/10.18280/acsm.480611.

[3] Kalendova A., Kupkova J., Urbaskova M., Merinska D., Applications of clays in nanocomposites and ceramics, Minerals, 2024, 14, 93, https://doi.org/10.3390/min14010093.

[4] Lysenkov E., Klepko V., Bulavin L., Lebovka N., Physicochemical properties of Laponite®/polyethylene oxide-based composites, Chem Rec, 2024, 24, e202300166, https://doi.org/10.1002/tcr.202300166.

[5] Qian Y., Huang Z., Zhou G., Chen C., Sang Y., Yu Z., Jiang L., Mei Y., Wei Y., Preparation and properties of organically modified Na-montmorillonite, Materials, 2023, 16, 3184, https://doi.org/10.3390/ma16083184.
[6] Wang R., Li H., Ge G., Dai N., Rao J., Ran H., Zhang Y., Montmorillonite-based two-dimensional nanocomposites: Preparation and applications, Molecules, 2021, 26, 2521, https://doi.org/10.3390/molecules26092521.
[7] Mapossa A.B., da Silva Júnior A.H., de Oliveira C.R.S., Mhike W., Thermal, morphological and mechanical properties of multifunctional composites based on biodegradable polymers/bentonite clay: A review, Polymers, 2023, 15, 3443, https://doi.org/10.3390/polym15163443.
[8] Zhu T.T., Zhou C.H., Kabwe F.B., Wu Q.Q., Li C.S., Zhang J.R., Exfoliation of montmorillonite and related properties of clay/polymer nanocomposites, Appl Clay Sci, 2019, 169, 48–66, https://doi.org/10.1016/j.clay.2018.12.006.
[9] Lebovka N.I., Lysenkov E.A., Goncharuk A.I., Gomza Y.P., Klepko V.V., Boiko Y.P., Phase behavior, microstructure and percolation of PEG-1000 filled by multiwalled carbon nanotubes and organophilic montmorillonite, J Compos Mater, 2011, 45, 2555–2566, https://doi.org/10.1177/0021998311401107.
[10] Ali N., Chipara D., Lozano K., Hinthorne J., Chipara M., Polyethylene oxide–fullerene nanocomposites, Appl Surf Sci, 2017, 421, 220–227, https://doi.org/10.1016/j.apsusc.2016.11.166.
[11] Lee J., Kim B.S., Recent progress in poly(ethylene oxide)-based solid-state electrolytes for lithium-ion batteries, Bull Korean Chem Soc, 2023, 44, 831–840, https://doi.org/10.1002/bkcs.12767.
[12] Reda H., Tanis I., Harmandaris V., Distribution of mechanical properties in poly(ethylene oxide)/silica nanocomposites via atomistic simulations: From the glassy to the liquid state, Macromolecules, 2024, 57, 3967–3984, https://doi.org/10.1021/acs.macromol.4c00537.
[13] Lysenkov E., Melnyk I., Bulavin L., Klepko V., Lebovka N., Structure of polyglycols doped by nanoparticles with anisotropic shape, In: Bulavin L., Lebovka N. (eds), Physics of Liquid Matter: Modern Problems, 2015, 171, 165–198, https://doi.org/10.1007/978-3-319-20875-6_7.
[14] Popov I., Cheng S., Sokolov A.P., Broadband dielectric spectroscopy and its application in polymeric materials, In: Macromolecular Engineering, 2022, 1–39, https://doi.org/10.1002/9783527815562.mme0059.
[15] Wang Q., Che J., Wu W., Hu Z., Liu X., Ren T., Chen Y., Zhang J., Contributing factors of dielectric properties for polymer matrix composites, Polymers, 2023, 15, 590, https://doi.org/10.3390/polym15030590.
[16] Sengwa R.J., Choudhary S., Sankhla S., Dielectric properties of montmorillonite clay filled poly(vinyl alcohol)/poly(ethylene oxide) blend nanocomposites, Compos Sci Technol, 2010, 70, 1621–1627, https://doi.org/10.1016/j.compscitech.2010.06.003.
[17] Anwar N., Ishtiaq M., Shakoor A., Niaz N.A., Rizvi T.Z., Qasim M., Irfan M., Mahmood A., Dielectric properties of polymer/clay nanocomposites, Polym Polym Compos, 2021, 29, 807–813, https://doi.org/10.1177/0967391120953250.
[18] Noda N., Lee Y.H., Bur A.J., Prabhu V.M., Snyder C.R., Roth S.C., McBrearty M., Dielectric properties of nylon 6/clay nanocomposites from on-line process monitoring and off-line measurements, Polymer, 2005, 46, 7201–7217, https://doi.org/10.1016/j.polymer.2005.06.046.
[19] Li X., Xu M., Zhang K., Xie D., Cao X., Liu X., Influence of organic intercalants on the morphology and dielectric properties of XLPE/montmorillonite nanocomposite dielectrics, IEEE Trans Dielectr Electr Insul, 2014, 21, 1705–1717, https://doi.org/10.1109/TDEI.2014.004317.
[20] Lysenkov E., Klymenko L., Determining the effect of dispersed aluminum particles on the functional properties of polymeric composites based on polyvinylidene fluoride, East Eur J Enterp Technol, 2021, 3, 59–66, https://doi.org/10.15587/1729-4061.2021.228731
[21] Li Z., Fu J., Zhou X., Gui S., Wei L., Yang H., Li H., Guo X., Ionic conduction in polymer-based solid electrolytes, Adv Sci, 2023, 10, e2201718, https://doi.org/10.1002/advs.202201718.
[22] Tsonos C., Exploring the high frequencies AC conductivity response in disordered materials by using the damped harmonic oscillator, J Compos Sci, 2022, 6, 200, https://doi.org/10.3390/jcs6070200.
[23] Greenhoe B.M., Hassan M.K., Wiggins J.S., Mauritz K.A., Universal power law behavior of the AC conductivity versus frequency of agglomerate morphologies in conductive carbon nanotube-reinforced epoxy networks, J Polym Sci B Polym Phys, 2016, 54, 1918–1923, https://doi.org/10.1002/polb.24121.
[24] Buketov A., Smetankin S., Lysenkov E., Yurenin K., Akimov O., Yakushchenko S., Lysenkova I., Electrophysical properties of epoxy composite materials filled with carbon black nanopowder, Adv Mater Sci Eng, 2020, 2020, 6361485, https://doi.org/10.1155/2020/6361485.
[25] Moreno M., Quijada R., Santa Ana M.A., Benavente E., Gomez-Romero P., González G., Electrical and mechanical properties of poly(ethylene oxide)/intercalated clay polymer electrolyte, Electrochim Acta, 2011, 58, 112–118, https://doi.org/10.1016/j.electacta.2011.08.096.
[26] Lysenkov E., Bilyi S., Nesin S., Klepko V., Influence of preparation conditions on structure and properties of composites based on polyethylene oxide and clay nanoparticles, In: 2023 IEEE 13th International Conference on Electronics and Information Technologies (ELIT), IEEE, 2023, 325–329, https://doi.org/10.1109/ELIT61488.2023.10310721.
[27] Lysenkov E.A., Strutskyi O.V., Structure and functional properties of nanocomposites based on polyethylene oxide and silver nanoparticles, In: Fesenko O., Yatsenko L. (eds), Nanostructured Surfaces, Nanocomposites and Nanomaterials, and Their Applications, 2023, 296, 245–265, https://doi.org/10.1007/978-3-031-42704-6_18.
[28] Zhu Y., Kottarath S., Iroh J.O., Vaia R.A., Progressive intercalation and exfoliation of clay in polyaniline–montmorillonite clay nanocomposites and implication to nanocomposite impedance, Energies, 2022, 15, 5366, https://doi.org/10.3390/en15155366.
[29] Lysenkov E.A., Klepko V., Lazarenko M.M., Structure-properties relationships of nanocomposites based on polyethylene oxide and anisometric nanoparticles, In: Fesenko O., Yatsenko L. (eds), Nanomaterials and Nanocomposites, Nanostructure Surfaces, and Their Applications, Springer Proceedings in Physics, 2023, 279, 409–437, https://doi.org/10.1007/978-3-031-18096-5_25.
[30] Tuncer E., Gubański S.M., Nettelblad B., Dielectric relaxation in dielectric mixtures: Application of the finite element method and its comparison with dielectric mixture formulas, J Appl Phys, 2001, 89, 8092–8100,

https://doi.org/10.1063/1.1372363.
[31] Hirschorn B., Orazem M.E., Tribollet B., Vivier V., Frateur I., Musiani M., Determination of effective capacitance and film thickness from constant-phase-element parameters, Electrochim Acta, 2010, 55, 6218–6227, https://doi.org/10.1016/j.electacta.2009.10.065.
[32] Singh A., Kumar D., Thakur A., Gupta N., Shinde V., Saini B.S., Kaur R., Galvanostatic deposition of manganese oxide films for super capacitive application and their fractal analysis, Ionics, 2021, 27, 2193–2202, https://doi.org/10.1007/s11581-021-03966-6.
[33] Drakopoulos S.X., Wu J., Maguire S.M., Srinivasan S., Randazzo K., Davidson E.C., Priestley R.D., Polymer nanocomposites: Interfacial properties and capacitive energy storage, Prog Polym Sci, 2024, 156, 101870, https://doi.org/10.1016/j.progpolymsci.2024.101870.
[34] Romanini M., Macovez R., Valenti S., Noor W., Tamarit J.L., Dielectric spectroscopy studies of conformational relaxation dynamics in molecular glass-forming liquids, Int J Mol Sci, 2023, 24, 17189, https://doi.org/10.3390/ijms242417189.